PAPER

Check for updates

Absolute and relative-rate measurement of the rate coefficient for reaction of perfluoro ethyl vinyl ether (C$_2$F$_5$OCF=CF$_2$) with OH

G. Srinivasulu, A. J. C. Bunkan, D. Amedro and J. N. Crowley [ID] *

The rate coefficient (k_1) for the reaction of OH radicals with perfluoro ethyl vinyl ether (PEVE, C$_2$F$_5$OCF=CF$_2$) has been measured as a function of temperature (T = 207–300 K) using the technique of pulsed laser photolysis with detection of OH by laser-induced fluorescence (PLP-LIF) at pressures of 50 or 100 Torr N$_2$ bath gas. In addition, the rate coefficient was measured at 298 K and in one atmosphere of air by the relative-rate technique with loss of PEVE and reference reactant monitored *in situ* by IR absorption spectroscopy. The rate coefficient has a negative temperature dependence which can be parameterized as: $k_1(T)$ = 6.0 × 10^{-13} exp[(480 ± 38/T)] cm^3 molecule^{-1} s^{-1} and a room temperature value of k_1 (298 K) = (3.0 ± 0.3) × 10^{-12} cm^3 molecule^{-1} s^{-1}. Highly accurate rate coefficients from the PLP-LIF experiments were achieved by optical on-line measurements of PEVE and by performing the measurements at two different apparatuses. The large rate coefficient and the temperature dependence indicate that the reaction proceeds *via* OH addition to the C=C double bond, the high pressure limit already being reached at 50 Torr N$_2$. Based on the rate coefficient and average OH levels, the atmospheric lifetime of PEVE was estimated to be a few days.

1 Introduction

Desirable properties such as thermal and chemical resistance have led to the use of fluoropolymers in many industrial processes including the production of plastics, elastomers or membranes[1,2] and to their production in large quantities. The most important commercial fluoropolymers are homopolymers based on only three main monomers; tetrafluoroethylene (TFE), vinyl fluoride and vinylidene fluoride.[3] In addition, smaller amounts of co-polymers with tailored properties are made with co-monomers like hexafluoropropylene and perfluoro vinyl ethers.

Since perfluorinated compounds generally have strong absorption features in the atmospheric infrared window and often have long atmospheric lifetimes, many of them are very potent greenhouse gases.[4–6] To evaluate their impact on climate change, accurate assessment of their atmospheric sinks is essential. From a physical chemical perspective, we note that the reaction kinetics of perfluoro substituted organic trace gases can differ greatly from the non-fluorinated analogues. Study of the OH reaction with a fluorinated ethyl vinyl ether (electrophilic addition of OH to the C=C double bond) allows us to analyse the electronic effects caused by the presence of a fluorinated alkyl

group separated from the electron rich double bond by the ether linkage.

To the best of our knowledge, there are no published studies on the atmospheric fate of perfluoro ethyl vinyl ether (C$_2$F$_5$OCF=CF$_2$, henceforth PEVE) though a few experimental studies on related reactions of perfluoro methyl vinyl ether[7–9] and perfluoro propyl vinyl ether[10] exist. In this work we have studied the kinetics of the reaction of PEVE with OH radicals (R1) using both the technique of pulsed laser photolysis with detection of OH radicals by laser-induced fluorescence as well as relative-rate measurements using FTIR detection of reactants to derive the rate coefficient, k_1.

$$OH + PEVE \rightarrow products \qquad (R1)$$
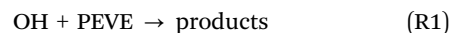
2 Experimental methods

Both absolute and relative-rate methods were used to determine the rate coefficient, k_1, for the title reaction.

2.1 Pulsed laser photolysis, laser-induced fluorescence (PLP-LIF)

Absolute rate coefficients were determined using the pulsed laser photolysis, laser-induced fluorescence technique with two different experimental set-ups (PLP-LIF1 and PLP-LIF2).

Division of Atmospheric Chemistry, Max-Planck-Institut für Chemie, 55128 Mainz, Germany. E-mail: john.crowley@mpic.de

This journal is © the Owner Societies 2018
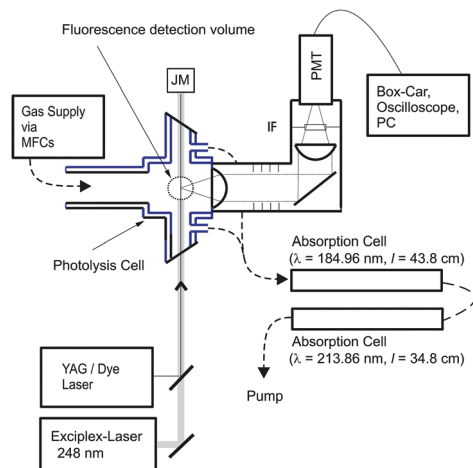
Phys. Chem. Chem. Phys., 2018, **20**, 3761–3767 | 3761

Fig. 1 Experimental setup (PLP-LIF1) for the absolute measurements of $k_1(T)$. MFC = mass flow controller, JM = joule meter, PMT = photomultiplier tube, IF = interference filter.

The one used for most of the measurements (PLP-LIF1), is shown in Fig. 1. This apparatus has been described in detail elsewhere[11] and only a brief description will be given here. The quartz reaction cell has a volume of ≈ 500 cm^3 and can be thermostatted to the desired temperature by circulating ethanol through its jacket. The measurements were performed at temperatures between 207 and 300 K at pressures of 50 and 100 Torr N$_2$ and 10 Hz laser repetition rate. The gas flow, regulated using calibrated mass flow controllers (MKS), was chosen to ensure that a fresh gas mixture was available for each laser pulse.

When using PLP-LIF1, OH radicals were generated by pulsed photolysis of H$_2$O$_2$ or HNO$_3$ at 248 nm using an exciplex laser (LambdaPhysik 300i).

$$H_2O_2 + h\nu \rightarrow 2OH \quad (R2)$$

$$HNO_3 + h\nu \rightarrow OH + NO_2 \quad (R3)$$
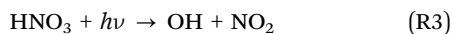
The concentrations of H$_2$O$_2$ (1–2 × 10^{14} molecule cm^{-3}) and HNO$_3$ (4–6 × 10^{14} molecule cm^{-3}) were measured by on-line optical absorption at 213.86 nm and 184.95 nm, respectively using low pressure Zn and Hg lamps as light sources. By analogy to PPVE,[10] PEVE does not absorb significantly at 213.86 nm. Laser fluences of 10–20 mJ cm^{-2} per pulse resulted in OH radical concentrations of (1–2) × 10^{11} molecule cm^{-3}. OH was monitored in real time *via* its laser-induced fluorescence after exciting the A$^2\Sigma(v=1) \leftarrow$ X$^2\Pi(v=0)$, Q$_{11}$(1) transition at ≈ 282 nm using a frequency-doubled, YAG-pumped Dye-Laser (Quantel Brilliant B plus Lambda-Physik ScanMate II). OH fluorescence was detected using a photomultiplier screened with a 310 nm interference filter. The photomultiplier signal was accumulated using a box-car integrator (Stanford Research Systems, SR 250).

The other absolute measurements were performed on a similar apparatus (PLP-LIF2) in our laboratory,[12] which is equipped for both LIF and transient absorption spectroscopy detection schemes. The LIF detection of OH was similar to that described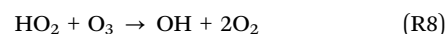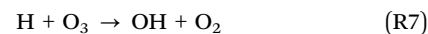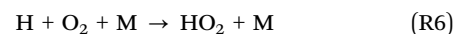 above, where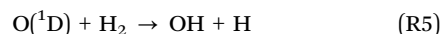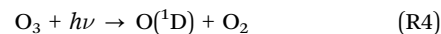as OH radicals were generated from H$_2$O$_2$ in (R2) using the pulsed, 266 nm emission of a frequency quadrupled Nd:YAG laser (Quantel Brilliant B).

When H$_2$O$_2$ was used as OH precursor, the concentration of PEVE was measured in both experimental setups by on-line optical absorption at 184.95 nm using the cross-section determined in this study. Optically derived concentrations of PEVE agreed to within $\approx 10\%$ with those calculated from its mixing ratio in the storage bulb and the partial flow and pressure.

Optical measurements of PEVE were not possible when using HNO$_3$ as OH precursor owing to very large optical extinction due to HNO$_3$ absorption at this wavelength. Instead, PEVE concentrations were calculated from partial flows and the total pressure and cross calibrated against optical measurements in the absence of HNO$_3$.

2.2 Relative-rate measurements

The rate coefficient for the reaction of PEVE with OH radicals was measured in a 44 l cylindrical quartz reaction chamber equipped with White-type multi-pass optics providing a 43.7 m optical path length for infrared absorption spectroscopy.[13] The reactor was operated at 298 K and 1 bar total pressure. Six, external, radially mounted, UV photolysis lamps (30 W, emitting predominantly at 253.65 nm) provided a homogeneous light flux within the reactor for radical generation which was initiated by the photolysis of ozone in a large excess of hydrogen:

$$O_3 + h\nu \rightarrow O(^1D) + O_2 \quad (R4)$$

$$O(^1D) + H_2 \rightarrow OH + H \quad (R5)$$

$$H + O_2 + M \rightarrow HO_2 + M \quad (R6)$$

$$H + O_3 \rightarrow OH + O_2 \quad (R7)$$

$$HO_2 + O_3 \rightarrow OH + 2O_2 \quad (R8)$$

OH precursor concentrations were: (2.2–10.4) × 10^{14} molecule cm^{-3} O$_3$ and (0.1–1.7) × 10^{17} molecule cm^{-3} H$_2$. Infrared spectra (500–3500 cm^{-1}) of PEVE and a reference trace gas were recorded at a resolution of 0.5 cm^{-1} with a Bruker Vector FTIR instrument with MCT detector.

2.3 Chemicals

N$_2$ (Westfalen 99.999%), H$_2$ (Westfalen 99.999%), synthetic air (Westfalen), propane (Linde, 99.95%) and PEVE (Merck, 99%) were used as supplied without further purification. H$_2$O$_2$ (AppliChem, 50 wt%) was concentrated to > 90 wt% by vacuum distillation. Anhydrous nitric acid was prepared by mixing KNO$_3$ (Sigma Aldrich, 99%) and H$_2$SO$_4$ (Roth, 98%), and condensing HNO$_3$ vapour into a liquid nitrogen trap. To prevent decomposition the nitric acid sample was stored at −17 °C between the measurements. O$_3$ was generated by photodissociation of O$_2$, achieved by passing air over a low pressure Hg-lamp emitting at 184.95 nm.

3762 | *Phys. Chem. Chem. Phys.*, 2018, **20**, 3761–3767

This journal is © the Owner Societies 2018

3 Results

3.1 Absorption cross-section of PEVE at 184.95 nm

To accurately determine the concentration of PEVE in the PLP-LIF measurements, the cross-section at 184.95 nm was required. The optical densities (OD) measured at various pressures (1.67–107.0 Torr) of accurately diluted mixtures of PEVE in N_2 are shown in Fig. 2. The absorption cross-section, obtained by dividing the slope of a plot of OD *vs.* [PEVE] by the optical path length, yielded $\sigma_{184.95\,nm} = (5.61 \pm 0.02) \times 10^{-18}$ cm^2 molecule^{-1} where the errors are 2σ statistical only. The total uncertainty is estimated to be 5% to give a final value of $(5.61 \pm 0.28) \times 10^{-18}$ cm^2 molecule^{-1} which is very close to that previously measured for perfluoro propyl vinyl ether.[10] Experiments were conducted using several different sample mixtures to check for systematic errors. The cross-sections obtained were identical within the precision of the measurement.

3.2 Absolute rate coefficients (207–300 K)

In the PLP-LIF1 and PLP-LIF2 set-ups, the rate coefficient for the reaction of PEVE with OH radicals was measured under pseudo-first order conditions with [PEVE] $\gg$ [OH]$_0$. The OH radical time profiles are then given by

$$[\text{OH}]_t = [\text{OH}]_0 \exp(-[k_1[\text{PEVE}]+ k_d]t) \tag{i}$$

where k_1 is the bimolecular rate coefficient for the reaction of PEVE with OH radicals and k_d is the pseudo-first order rate coefficient for other OH loss processes, mainly reaction with the precursor and diffusion/advection out of the detection zone.

The OH-LIF time profiles were fitted to eqn (i) and example profiles from measurements at 298 K obtained using PLP-LIF1 are shown in Fig. 3. Each measured OH-LIF time profile is the average of 20–25 measurements and was mono-exponential over at least two orders of magnitude. Rate coefficients for the reaction of OH with PEVE were obtained by linear fitting of the pseudo-first order rate coefficients as a function of [PEVE], as shown in Fig. 4. The rate coefficients and the experimental
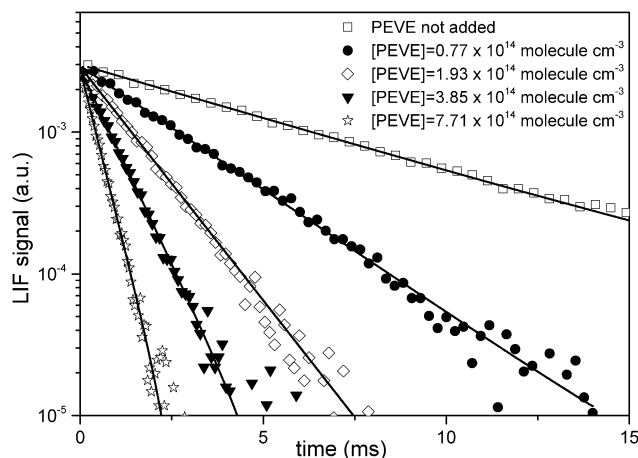

Fig. 3 OH decays in the presence of various concentrations of PEVE at p = 50 Torr and T = 298 K. HNO$_3$ photolysis at 248 nm was used as OH source.
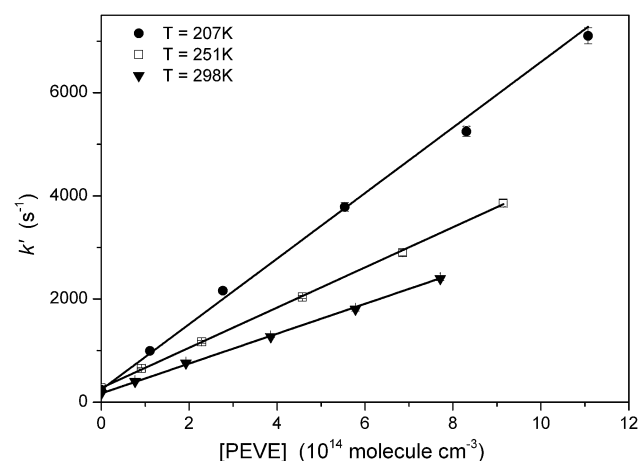

Fig. 4 Plot of pseudo first-order rate coefficient (k') *versus* [PEVE] at a total pressure of 50 Torr N$_2$ and at three different temperatures. The data were obtained using the PLP-LIF1 set-up and with photolysis of HNO$_3$ as the OH precursor. The error bars represent 2σ statistical uncertainty and in several cases are smaller than the symbol.

conditions used (temperature, pressure and OH-precursor) are summarised in Table 1.

Values of k_1 obtained with the two experimental setups and using different OH precursors show no significant difference and no dependence on pressure between 50 and 100 Torr N$_2$. The rate coefficient does however show a significant, negative temperature dependence.

3.3 Relative rate coefficients

In the relative-rate experiments, the loss of PEVE was measured relative to that of propane. Propane was chosen as a reference because it does not react with other compounds in the reaction mixture, does not stick to surfaces and it has a well-established rate coefficient. In the absence of loss processes other than reaction with OH, the depletion factors, ln(initial concentration/concentration after time t), for reactant and reference are
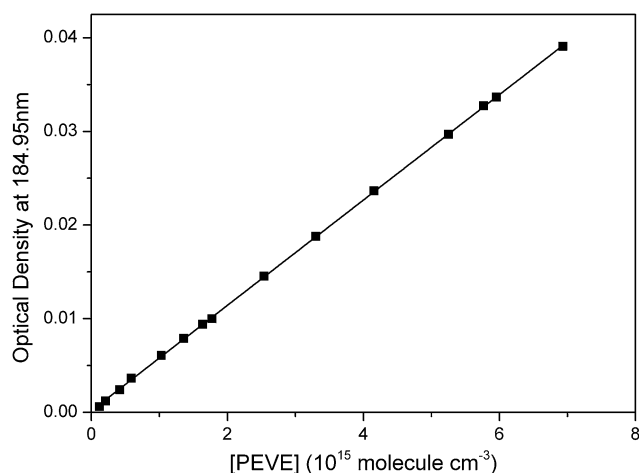

Fig. 2 Beer–Lambert plot of optical density measured at 184.95 nm *versus* concentration of PEVE. The effective absorption cross-section of PEVE at 184.95 nm is $\sigma_{184.95nm} = (5.61 \pm 0.28) \times 10^{-18}$ cm^2 molecule^{-1} including uncertainty from dilution and pressure measurements.

This journal is © the Owner Societies 2018

Phys. Chem. Chem. Phys., 2018, **20**, 3761–3767 | 3763

Table 1 Rate coefficients and experimental conditions for the reaction of OH with PEVE from PLP-PLIF experiments

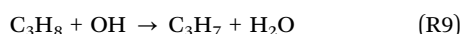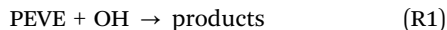| Setup	Temp. (K)	OH precursor	Pressure (Torr)	$k_1(T)^a$ (10^{-12} cm^3 molecule^{-1} s^{-1})
PLP-LIF1	207	HNO$_3$	50	6.35 ± 0.30
PLP-LIF1	225	HNO$_3$	50	5.32 ± 0.31
PLP-LIF1	233	HNO$_3$	50	4.59 ± 0.05
PLP-LIF1	251	HNO$_3$	50	3.90 ± 0.07
PLP-LIF1	260	H$_2$O$_2$	50	3.85 ± 0.20
PLP-LIF1	268	H$_2$O$_2$	50	3.49 ± 0.12
PLP-LIF1	270	HNO$_3$	50	3.39 ± 0.08
PLP-LIF1	272	H$_2$O$_2$	100	3.60 ± 0.12
PLP-LIF1	280	H$_2$O$_2$	100	3.24 ± 0.09
PLP-LIF1	281	H$_2$O$_2$	50	3.22 ± 0.12
PLP-LIF1	299	HNO$_3$	50	2.90 ± 0.07
PLP-LIF1	299	H$_2$O$_2$	50	3.04 ± 0.05
PLP-LIF1	298	H$_2$O$_2$	100	3.03 ± 0.03
PLP-LIF2	299	H$_2$O$_2$	50	3.02 ± 0.04
PLP-LIF2	300	H$_2$O$_2$	50	2.95 ± 0.15
PLP-LIF2	300	H$_2$O$_2$	50	2.96 ± 0.14
PLP-LIF2	300	H$_2$O$_2$	50	2.70 ± 0.14
PLP-LIF2	300	H$_2$O$_2$	100	2.75 ± 0.04

^{a} Uncertainty in k_1 is 2σ statistical only.

described by:

$$\ln\left(\frac{[\text{PEVE}]_0}{[\text{PEVE}]_t}\right) = \frac{k_1}{k_9} \ln\left(\frac{[\text{propane}]_0}{[\text{propane}]_t}\right) \qquad (\text{ii})$$

where $[\text{PEVE}]_0$, $[\text{propane}]_0$, $[\text{PEVE}]_t$ and $[\text{propane}]_t$ are the concentrations of PEVE and propane at times zero and t respectively, and k_1 and k_9 are the rate coefficients of reactions (1) and (9).

$$\text{PEVE} + \text{OH} \rightarrow \text{products} \qquad (\text{R1})$$

$$\text{C}_3\text{H}_8 + \text{OH} \rightarrow \text{C}_3\text{H}_7 + \text{H}_2\text{O} \qquad (\text{R9})$$

The initial concentration ranges used for PEVE and propane were $(1.0–3.3) \times 10^{13}$ molecule cm^{-3} and $(1.0–4.0) \times 10^{14}$ molecule cm^{-3}, respectively. A typical experiment lasted around one hour, with the photolysis lamps switched on for 5–10 periods of 10–300 s duration for each experiment. The intermittent acquisition of FTIR spectra (64 scans at 0.5 cm^{-1} resolution) took ≈ 2 min. No significant loss of either PEVE or propane on these time scales was observed in the reaction mixtures including O$_3$ and H$_2$ in the dark.

The time dependent depletion factors for PEVE and propane were obtained by least squares fitting to a reference spectrum in the range 1080–1360 cm^{-1} for PEVE and 2810–2920 cm^{-1} for propane. Absorption by products was accounted for by including qualitative reference spectra of the assumed products, CF$_2$O, (FCO)$_2$ and C$_2$F$_5$OCFO in a spectral fitting procedure using DOASIS software.[14] An example spectrum with fit and residuals is shown in Fig. 5.

Assuming that the photo-oxidation mechanism for PEVE is similar to those of PMVE and PPVE, perfluoro methoxy radicals (CF$_3$O) are expected to be formed in our experiments. These are known to react with hydrocarbons[15] and may, in principle, influence our measurements. To assess the potential systematic bias due to reactions of the CF$_3$O radical, as well as possible interferences from O(^{1}D) reactions with PEVE or propane the concentration of H$_2$, a scavenger of both CF$_3$O and O(^{1}D), was
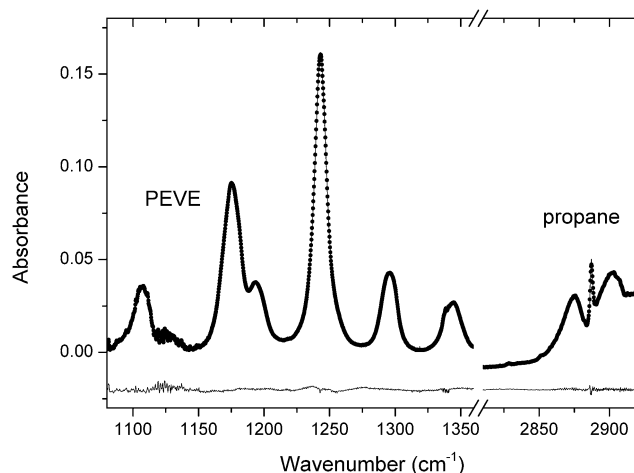
Fig. 5 Spectral range used in the analysis of the relative-rate experiments with recorded spectrum (symbols), fitted reference spectrum (full line) and fit residual (offset by -0.02 absorbance units).

varied by an order of magnitude. As illustrated in Fig. 6 and Table 2, there was no discernible impact on the relative decay rate of PEVE and propane and we conclude that any bias is too small to be significant. In support of this conclusion, numerical simulations[16] were carried out which used a literature rate coefficient for the reaction of CF$_3$O with propane and one for CF$_3$O + H$_2$ which was taken to be the same as OH + H$_2$ (6.7×10^{-15} cm^3 molecule^{-1} s^{-1} at 298 K).[17] The rate coefficient for CF$_3$O + H$_2$ is actually likely to be larger as the CF$_3$O radical is more reactive than OH radicals towards hydrocarbons.[15] The simulations revealed that the reaction of perfluoro methoxy radicals with propane accounts for only 2% of the total propane loss even at the lowest H$_2$ concentrations, which is in accord with our observations. A total of four relative-rate experiments were performed under different experimental conditions, which are summarised in Table 2 and Fig. 6. The values of k_1/k_9 from the single experiments agree within 10% but we may discern a weak,
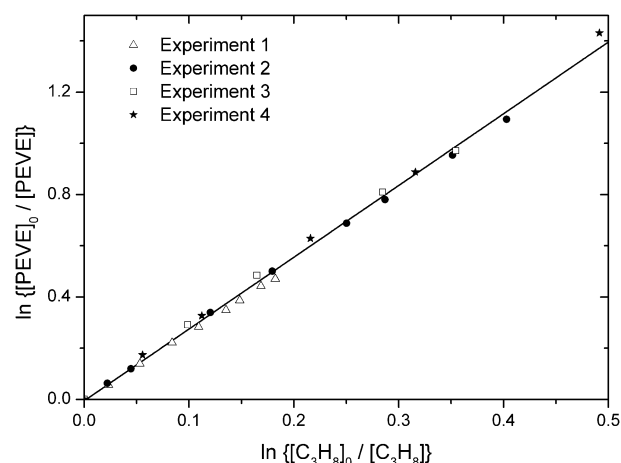
Fig. 6 Fractional loss of PEVE and propane in the presence of OH radicals from four individual experiments in 750 Torr air diluent. The conditions for each experiment are listed in Table 2.

3764 | *Phys. Chem. Chem. Phys.*, 2018, **20**, 3761–3767

This journal is © the Owner Societies 2018

Table 2 Summary of experimental conditions in the relative rate study

Expt. no.	P (Torr)	$[PEVE]_0{}^a$	$[C_3H_8]_0{}^a$	$[O_3]_0{}^a$	$[H_2]_0{}^b$	$[OH]_0{}^c$	$k_1/k_9{}^d$
1	750	3.3	39.8	22.1	0.36	3.22	2.604 ± 0.032
2	750	2.7	22.0	36.3	0.29	6.78	2.713 ± 0.030
3	750	1.6	12.7	58.1	1.7	1.55	2.752 ± 0.108
4	750	1.0	10.1	103.8	0.13	1.80	2.847 ± 0.042

^{a} The initial concentrations of PEVE, C_3H_8 and O_3 (units of 10^{13} molecule cm^{-3}) were determined from the IR spectra. ^{b} The H_2 concentration (units of 10^{17} molecule cm^{-3}) was derived from pressure measurements. ^{c} The OH concentration (units of 10^8 molecule cm^{-3}) from the initial decay of PEVE. ^{d} Uncertainty is 2σ statistical only.

barely significant positive dependence of the relative rate coefficient on the O_3 concentration. *i.e.* k_1/k_9 changes (by $\approx$ 9%) from 2.604 ± 0.032 to 2.847 ± 0.042 going from the lowest to highest ozone concentration used. Potential explanations for this would be reaction of either O_3 or $O(^3P)$ with PEVE, whereby $O(^3P)$ is formed in the collisional quenching of $O(^1D)$ (formed in (R5)) with bath gas. Numerical simulations revealed that the ratio of $O(^3P)$/OH concentrations varied from $\approx$ 0.01 to 0.1 between experiments, but this was not accompanied by a significant change in the relative rate constant. We also note that the dark loss of PEVE in the presence of O_3 was too small to explain this effect. We have no robust explanation of this weak trend and increase the errors on the rate coefficient obtained by the relative-rate method to take this into account.

A linear least squares fit to all data (solid line in Fig. 6) gives $k_1/k_9 = 2.802 \pm 0.061$ (2σ). From this k_1 can be determined using an evaluated literature value of $k_9 = (1.1 \pm 0.08) \times 10^{-12}$ cm^3 molecule^{-1} s^{-1} [18] to give $k_1 = (3.1 \pm 0.35) \times 10^{-12}$ cm^3 molecule^{-1} s^{-1} at 298 K and 1 bar total pressure of air, where the uncertainty contains both statistical and systematic errors originating from the uncertainty (7%) in the literature value for k_9 and also the potential bias (<10%) related to the presence of O_3.

4 Discussion and literature comparison

The complete dataset, including data obtained using two different experimental setups for determination of the absolute rate coefficient and also the relative rate study is summarised in Fig. 7 as an Arrhenius plot. The room temperature (298 $\pm$ 2 K) rate coefficients obtained are $k_1 = (2.97 \pm 0.30)$ cm^3 molecule^{-1} s^{-1} (PLP-LIF1, 50 Torr N_2), $k_1 = (2.90 \pm 0.29)$ cm^3 molecule^{-1} s^{-1} (PLP-LIF2, 50–100 Torr N_2) and $k_1 = (3.1 \pm 0.35)$ cm^3 molecule^{-1} s^{-1} (relative rate, 750 Torr air). The uncertainties reported for the absolute rate coefficients are dominated by estimated uncertainty in the PEVE cross-section.

The three results are thus in very good agreement, confirming that k_1 is independent of bath gas identity (N_2 or air) or pressure between 50 and 750 Torr. Combining all three sets of data at room temperature we derive $k_1(298 K) = (3.0 \pm 0.3) \times 10^{-12}$ cm^3 molecule^{-1} s^{-1} where the uncertainty is dominated

by potential systematic errors in both absolute and relative-rate experiments.

The temperature dependent data obtained using the PLP-LIF1 set-up can be described by an Arrhenius expression: k_1 (207–300 K) = $(5.9 \pm 0.8) \times 10^{-13}$ exp$[(480 \pm 38)/T]$ cm^3 molecule^{-1} s^{-1}, which was derived by instrument-weighted, least-squares fitting to the data displayed in Fig. 7. The negative temperature dependence stems from the formation of an association complex as described for other fluorinated, vinyl ethers.[10,23]

The quoted errors are 2σ (statistical only). We adopt the temperature dependence (480/T) and modify the pre-exponential factor slightly to give the average room temperature rate coefficient from all experiments and obtain: $k_1(200–300 K) = 6.0 \times 10^{-13}$ exp(480/T) for use in calculation of the rate coefficient at any temperature in the range listed, where the uncertainty will be 10%, independent of temperature.

In the following section, we compare our results with previous literature determinations of rate coefficients for the reactions of OH with perfluoro methyl vinyl ether (PMVE, $CF_3OCF{=}CF_2$) and perfluoro propyl vinyl ether (PPVE, $C_3F_7OCF{=}CF_2$) which differ from PEVE only in the length of the alkyl chain on the opposite side of the ether linkage to the double bond (CF_3 *versus* C_2F_5 *versus* C_3F_7).

Table 3 lists literature values for room temperature rate coefficients and Arrhenius parameters for the reactions of OH with PMVE, PEVE and PPVE. Note that Mashino *et al.*[8] measured the rate coefficient for PMVE with OH radicals relative to ethene and ethyne at 296 K in 700 Torr air, and they report a value of $(2.6 \pm 0.3) \times 10^{-12}$ cm^3 molecule^{-1}s^{-1}. By using their relative rate constants and the most recent IUPAC recommendations[18] for the ethene (7.8×10^{-12} cm^3 molecule^{-1}s^{-1}) and ethyne (7.5×10^{-12} cm^3 molecule^{-1} s^{-1}) reference reactions we recalculate this to be $(2.2 \pm 0.3) \times 10^{-12}$ cm^3 molecule^{-1} s^{-1}.
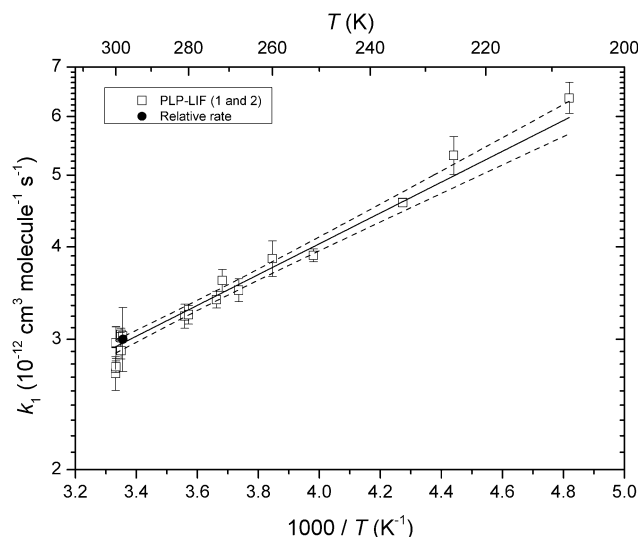
Fig. 7 Arrhenius plot of all data from the present study for the reaction between OH and PEVE. Open squares: PLP-LIF, filled circle: relative rate. The error bars represent 2σ statistical uncertainty. The solid line represents the Arrhenius expression: $k_1 = 5.9 \times 10^{-13}$ exp(480/T) cm^3 molecule^{-1} s^{-1}, the dashed lines are the 95% confidence intervals.

Table 3 Rate coefficients and Arrhenius parameters for the reactions of alkyl vinyl ethers with OH radicals

	k (298 K)[a]	A factor[b]	E_a[c]	Ref.
$CF_3OCF=CF_2$ (PMVE)	3.58 ± 0.46	641 ± 82	7.2 ± 0.3	(Li *et al.*, 2000)[7]
	2.2 ± 0.3[d]			(Mashino *et al.*, 2000)[8]
	2.98 ± 0.3[e]	10.1 ± 0.4	-2.7 ± 0.1	(Tokuhashi *et al.*, 2000)[9]
$CH_3OCH=CH_2$	33.5 ± 3.4			(Perry *et al.*, 1977)[19]
$C_2F_5OCF=CF_2$ (PEVE)	3.0 ± 0.3	6.0 ± 0.8	-4.0 ± 0.3	This work
$C_2H_5OCH=CH_2$	68 ± 7			(Thiault *et al.*, 2002)[20]
	77.9 ± 17.1			(Zhou *et al.*, 2006)[21]
$C_3F_7OCF=CF_2$ (PPVE)	3.4 ± 0.3	4.88 ± 0.49	-4.7 ± 0.1	(Amedro *et al.*, 2015)[10]
$C_3H_7OCH=CH_2$	110 ± 3.4			(Peirone *et al.*, 2011)[22]

[a] Units of 10^{-12} cm³ molecule⁻¹ s⁻¹. [b] Units of 10^{-13} cm³ molecule⁻¹ s⁻¹. [c] Units of kJ mol⁻¹. [d] Originally reported value has been corrected using the most recent IUPAC recommendations for the reference rate coefficients. [e] the authors stated that the overall uncertainty was less than 10%.

The rate coefficient measured in this work for PEVE is very similar to those reported using absolute techniques by Tokuhashi *et al.*[9] for PMVE and by Amedro *et al.*[10] for PPVE, both of whom report a room temperature rate coefficient close to 3–4 × 10⁻¹² cm³ molecule⁻¹ s⁻¹ and a weak, negative temperature dependence. Although the room temperature rate coefficient of Li *et al.*[7] obtained for PMVE is similar to these values, their large activation energy is inconsistent with the other experimental results and also with the fact that the reaction is expected to proceed *via* electrophilic addition of OH to the double bond of PMVE. As their experiments were conducted at a pressure of 1 Torr of He, where the high pressure limit is possibly not achieved, a lower room temperature rate coefficient may have been expected rather than a higher one. We have no explanation for this discrepancy, but note that low pressure studies of OH reactions often suffer from significant OH wall losses, and pulsed laser systems (essentially wall free) are expected to deliver more accurate results.

Considering only the datasets of Amedro *et al.*[10] Mashino *et al.*[8] and Tokuhashi *et al.*[9] we can discern a small increase in the rate coefficient with increasing chain length, although this is only just significant given the overall uncertainty reported by each experiment. The change in the negative activation energy is however more obvious, likely reflecting the formation of lower energy transition states on the exit channel to product formation for the larger association complexes formed from addition of OH to the vinyl ethers, though this has not been predicted by quantum chemical calculations for PMVE and PEVE.[10,23] Table 3 also lists room temperature rate coefficients for the reaction of non-fluorinated alkyl vinyl ethers. The rate coefficients for the non-fluorinated analogues are significantly larger by factors of 10 to 30 going from methyl–ethyl–propyl substituted alkyl vinyl ethers. As these are largely OH addition reactions,[24,25] this significant increase in the rate coefficient reflects the effect of increasing electron density at the double bond through donation from the alkoxy groups. This trend is clearly much weaker (if at all apparent) for the perfluorinated analogues, and may be expected given the more strongly bound electrons in the fluorinated alkyl/alkoxy groups.

The tropospheric lifetime of PEVE can be estimated by assuming uniform, global concentration of OH radicals. Using a value of [OH] $\approx 10^6$ molecule cm⁻³ [26] we estimate a tropospheric lifetime for PEVE due to its reaction with OH of ≈ 4 days. This is an order of magnitude shorter that the exchange time for transport to the stratosphere so that, like PPVE, PEVE will be, to a good approximation, completely degraded in the troposphere by reaction with OH. Since its lifetime is short, PEVE is unlikely to have a significant global warming potential. The atmospheric, OH-initiated degradation of PEVE is likely to lead to fluorinated oxygenates such as CF_2O and C_2F_5OCFO,[10,23] though this theoretical result awaits confirmation in experimental product studies, which are presently being undertaken in this laboratory.

5 Conclusions

The rate coefficient (k_1) of the reaction of OH with $C_2F_5OCF=CF_2$ (PEVE) has been measured for the first time. Both absolute and relative-rate methods at various pressures and temperatures were applied to derive a value of 6.0 × 10⁻¹³ exp(480/T) cm³ molecule⁻¹ s⁻¹ with a room temperature value of $(3.0 \pm 0.3) \times 10^{-12}$ cm³ molecule⁻¹ s⁻¹ independent of pressure in the range 50 to 100 Torr N₂. The use of three different production schemes for the OH radical, two different experimental set-ups for the pulsed laser experiments (50 or 100 Torr N₂) and relative rate constant measurements (750 Torr air) reduce the uncertainty on the rate coefficient to ≈ 10% at all temperatures. The values of k_1 obtained are consistent with rate coefficients for reaction of OH with other fluorinated vinyl ethers and significantly lower than measured for the non-fluorinated analogues. The large OH rate coefficient ensures that PEVE will not be a persistent fluorinated trace-gas in the atmosphere.

Conflicts of interest

There are no conflicts to declare.

Acknowledgements

3766 | *Phys. Chem. Chem. Phys.*, 2018, **20**, 3761–3767

This journal is © the Owner Societies 2018

Notes and references

1 A. E. Feiring, in *Organofluorine Chemistry: Principles and Commercial Applications*, ed. R. E. Banks, B. E. Smart and J. C. Tatlow, Springer, US, Boston, MA, 1994, pp. 339–372, DOI: 10.1007/978-1-4899-1202-2_16.

2 T. Hiyama and H. Yamamoto, in *Organofluorine Compounds: Chemistry and Applications*, ed. H. Yamamoto, Springer, Berlin, Heidelberg, 2000, pp. 183–233, DOI: 10.1007/978-3-662-04164-2_6.

3 S. Ebnesajjad, in *Applied Plastics Engineering Handbook*, William Andrew Publishing, Oxford, 2011, pp. 49–60, DOI: 10.1016/B978-1-4377-3514-7.10004-2.

4 M. K. W. Ko, N. D. Sze, W. C. Wang, G. Shia, A. Goldman, F. J. Murcray, D. G. Murcray and C. P. Rinsland, *J. Geophys. Res.: Atmos.*, 1993, **98**, 10499–10507.

5 M. J. Prather and J. Hsu, *Geophys. Res. Lett.*, 2008, **35**, L12810, DOI: 12810.11029/12008gl034542.

6 W. T. Sturges, T. J. Wallington, M. D. Hurley, K. P. Shine, K. Sihra, A. Engel, D. E. Oram, S. A. Penkett, R. Mulvaney and C. A. M. Brenninkmeijer, *Science*, 2000, **289**, 611–613.

7 Z. J. Li, Z. N. Tao, V. Naik, D. A. Good, J. C. Hansen, G. R. Jeong, J. S. Francisco, A. K. Jain and D. J. Wuebbles, *J. Geophys. Res.: Atmos.*, 2000, **105**, 4019–4029.

8 M. Mashino, M. Kawasaki, T. J. Wallington and M. D. Hurley, *J. Phys. Chem. A*, 2000, **104**, 2925–2930.

9 K. Tokuhashi, A. Takahashi, M. Kaise, S. Kondo, A. Sekiya and E. Fujimoto, *Chem. Phys. Lett.*, 2000, **325**, 189–195.

10 D. Amedro, L. Vereecken and J. N. Crowley, *Phys. Chem. Chem. Phys.*, 2015, **17**, 18558–18566.

11 M. Wollenhaupt, S. A. Carl, A. Horowitz and J. N. Crowley, *J. Phys. Chem.*, 2000, **104**, 2695–2705.

12 C. B. M. Groß, T. J. Dillon, G. Schuster, J. Lelieveld and J. N. Crowley, *J. Phys. Chem. A*, 2014, **118**, 974–985.

13 J. N. Crowley, G. Saueressig, P. Bergamaschi, H. Fischer and G. W. Harris, *Chem. Phys. Lett.*, 1999, **303**, 268–274.

14 S. Kraus, *DOASIS, DOAS intelligent system*, University of Heidelberg, 2006, https://doasis.iup.uni-heidelberg.de/bug tracker/projects/doasis/index.php.

15 S. B. Barone, A. A. Turnipseed and A. R. Ravishankara, *J. Phys. Chem.*, 1994, **98**, 4602–4608.

16 A. R. Curtis and W. P. Sweetenham, *FACSMILE/CHECKMAT User's Manual, AERE-R12805*, Atomic Energy Research Establishment, Harwell, 1988.

17 R. Atkinson, D. L. Baulch, R. A. Cox, J. N. Crowley, R. F. Hampson, R. G. Hynes, M. E. Jenkin, M. J. Rossi and J. Troe, *Atmos. Chem. Phys.*, 2004, **4**, 1461–1738.

18 R. Atkinson, D. L. Baulch, R. A. Cox, J. N. Crowley, R. F. Hampson, R. G. Hynes, M. E. Jenkin, M. J. Rossi and J. Troe, *Atmos. Chem. Phys.*, 2006, **6**, 3625–4055.

19 R. A. Perry, R. Atkinson and J. N. Pitts Jr., *J. Chem. Phys.*, 1977, **67**, 611–614.

20 G. Thiault, R. Thevenet, A. Mellouki and G. Le Bras, *Phys. Chem. Chem. Phys.*, 2002, **4**, 613–619.

21 S. Zhou, I. Barnes, T. Zhu, I. Bejan and T. Benter, *J. Phys. Chem. A*, 2006, **110**, 7386–7392.

22 S. A. Peirone, J. P. Aranguren Abrate, R. A. Taccone, P. M. Cometto and S. I. Lane, *Atmos. Environ.*, 2011, **45**, 5325–5331.

23 L. Vereecken, J. N. Crowley and D. Amedro, *Phys. Chem. Chem. Phys.*, 2015, **17**, 28697–28704.

24 B. Klotz, I. Barnes and T. Imamura, *Phys. Chem. Chem. Phys.*, 2004, **6**, 1725–1734.

25 S. Zhou, I. Barnes, T. Zhu, B. Klotz, M. Albu, I. Bejan and T. Benter, *Environ. Sci. Technol.*, 2006, **40**, 5415–5421.

26 R. G. Prinn, J. Huang, R. F. Weiss, D. M. Cunnold, P. J. Fraser, P. G. Simmonds, A. McCulloch, C. Harth, P. Salameh, S. O'Doherty, R. H. J. Wang, L. Porter and B. R. Miller, *Science*, 2001, **292**, 1882–1888.

This journal is © the Owner Societies 2018

Phys. Chem. Chem. Phys., 2018, **20**, 3761–3767 | 3767